

## Progress Towards a Physics Based Phenomenology of Intrinsic Rotation in H-mode and I-mode

J. Rice<sup>[1]\*</sup>, J. Hughes<sup>[1]</sup>, Z. Yan<sup>[5,2]</sup>, M. Xu<sup>[2]</sup>, G.R. Tynan<sup>[2]</sup>, P.H. Diamond<sup>[3,2]</sup>, Y. Kosuga<sup>[2]</sup>, T.S. Hahm<sup>[2,6]</sup>, Ö.D. Gürcan<sup>[4]</sup>, R. McDermott<sup>[7]</sup>, Y. Podpaly<sup>[1]</sup>, C.J. McDevitt<sup>[2]</sup>, C. Holland<sup>[2]</sup>, S.H. Müller<sup>[2]</sup>

<sup>[1]</sup>PSFC, MIT; <sup>[2]</sup>CMTFO, UCSD; <sup>[3]</sup>NFRI, Korea; <sup>[4]</sup>LPP, Ecole Polytechnique; <sup>[5]</sup>Dept. of Engr. Physics, UWM; <sup>[6]</sup>PPPL; <sup>[7]</sup>IPP, Garching, Germany

\* <rice@psfc.mit.edu>

**Abstract.** Recent progress towards a physics based phenomenology of intrinsic rotation in H-mode and I-mode is presented. In particular, we aim to elucidate the mechanism of the drive of intrinsic rotation by describing results from a synergistic combination of macroscopic experiments on Alcator C-Mod, microscopic experiments on the linear device CSDX, and theory. Results identify the edge (pedestal)  $\nabla T_i$  as the principle source of the drive for intrinsic rotation in C-Mod, and CSDX supports the hypothesis that turbulent residual stress is the mechanism coupling the edge gradient to plasma rotation. The unifying concept of the plasma as a heat engine is used to place the various elements of this investigation in context and to calculate the efficiency of rotation generation.

### 1. Introduction

Intrinsic toroidal rotation is important as a means for maintaining macroscopic stability to RWMs in the absence of NBI injection, and may also play a role in the dynamics of ITBs. Since the transport and relaxation of toroidal momentum is due to turbulence (n.b.  $\chi_\phi \sim \chi_i$ ), so intrinsic rotation necessarily implies the existence of an agent or element of the turbulent momentum flux which can work against turbulent viscosity. This off-diagonal flux is called the residual stress and is likely responsible for the self-acceleration of intrinsic flow. Residual stress may be understood as a momentum flux driven by  $\nabla P$ ,  $\nabla T$ ,  $\nabla n$  etc. which produces a directed macroscopic flow by converting radial inhomogeneity to broken  $k_{\parallel}$  symmetry of the fluctuation spectrum. This process resembles an engine, in that the turbulence converts thermodynamic free energy to macroscopic flow, just as a heat engine converts a temperature drop to useful work.

Several questions arise here. The first is concerned with the driving gradient. This is a subtle question, since the pressure gradient  $\nabla P$  can drive instabilities, break  $k_{\parallel}$  symmetry[1] by its contribution to  $\langle V_E \rangle'$ , and also quench turbulence[2] via  $\langle V_E \rangle'$ . Other possibilities include  $\nabla T$  and  $\nabla n$ . Here, we use comparison studies of H-mode and I-mode plasmas to identify the driving gradient. We then turn to microscopic fluctuation studies from the basic experiment CSDX to explicitly demonstrate both the existence of a fluctuation driven residual stress and its role in driving macroscopic rotation. Finally we describe a simple theory of the intrinsic rotation engine, based on entropy dynamics. This theory yields a simple figure of merit for the efficiency of the self-acceleration process.

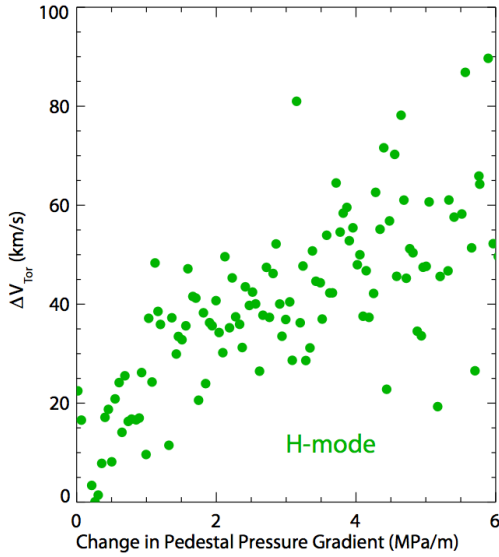


Figure 1: The change in the core rotation after the H-mode transition as a function of the pedestal pressure gradient.

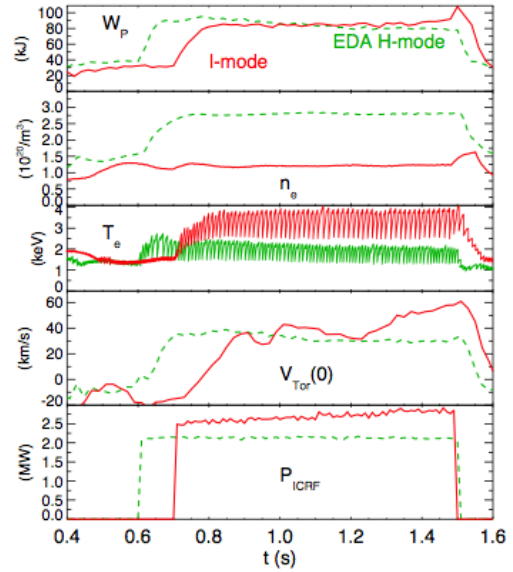


Figure 2: Time histories, from top to bottom, of the plasma stored energy, average electron density, central electron temperature, central rotation velocity and ICRF power, for an EDA H-mode (green dashed) and an I-mode (red) plasma.

## 2. Macroscopic: Alcator C-Mod

Studies of H-mode and I-mode[3] intrinsic rotation were conducted to identify the gradient which drives intrinsic rotation. The approach was to examine correlation between edge (pedestal) gradients with central rotation  $V_T(0)$ . The motivation is two fold – namely, to develop a phenomenology based on local parameters (in lieu of global scaling)[4] and to establish the edge  $\rightarrow$  core connection for intrinsic rotation. To this end, recall that intrinsic rotation has long been observed to originate at the edge.[5] Analysis of the data base indicates a good correlation between edge  $\nabla P$  and  $\Delta V_T(0)$  (the change in  $V_T(0)$  in through the transition) in C-Mod H-modes, as shown in Fig. 1. However, given the questions discussed above, we also explored correlations in I-mode. I-mode is an improved confinement regime which arises in states with unfavorable  $\nabla B$  drift which are slightly subcritical to the L $\rightarrow$ H bifurcation.[3] I-mode is notable for its steepened edge  $\nabla T$  with virtually no change in  $\nabla n$ , and thus is an ideal venue in which to separate edge  $\nabla T$  from edge  $\nabla P$ . A few general comments on I-mode follow.

First, I-mode exhibits enhanced intrinsic rotation, similar to Fig. 1. Note that the rise in  $V_T(0)$  follows the increase in stored energy  $W_p$ , as shown in Fig. 2. The upshot of this evolution is steepening of the edge temperature gradient (but not density gradient!), as shown in Fig. 3. As in H-mode, the rotation builds inward from the edge, as shown in Fig. 4. Note that the rise in  $v_T(0)$  clearly lags the rise in  $W_p$ . Given Figs. 2-4, it is no surprise that I-mode rotation exhibits a scaling of  $\Delta V_T(0) \sim \Delta W_p/I_p$ , i.e. change in

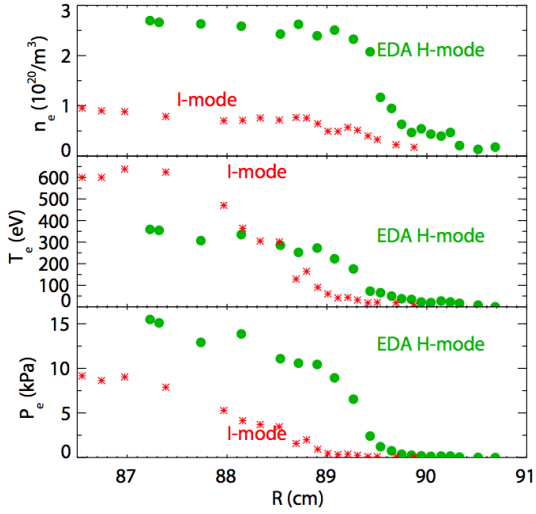


Figure 3: Edge profiles of the electron density (top frame), electron temperature (middle frame) and electron pressure (bottom frame) from the EDA H-mode (green dots) and the I-mode (red asterisks) discharges of Fig. 2.

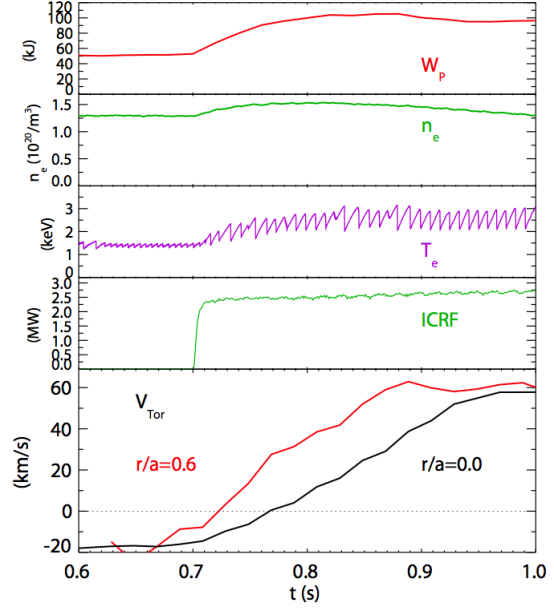


Figure 4: Parameter time histories for an I-mode discharge. In the bottom frame is the normalized chord-averaged toroidal rotation velocity from  $r/a = 0.6$  and  $r/a = 0.0$ .

central velocity tracks change in stored energy and is inversely proportional to current. This relation suggests a generation mechanism in which the plasma converts stored energy to directed flow kinetic energy, via the dynamics of turbulence.

To ‘differentially diagnose’ the drive, we compare  $\Delta V_T(0)$  vs  $\nabla P$  correlations in H-mode and I-mode. Fig. 5 shows a plot of  $\Delta V_T(0)$  vs  $\nabla P$  in I-mode. Note that in distinct contrast to Fig. 1 (for H-mode) the correlation of  $\Delta V_T(0)$  with  $\nabla P$  in I-mode is poor. This suggests that  $\nabla P$  is *not* the driver of intrinsic rotation in I-mode. Given this observation, we are naturally motivated to explore the correlation of  $\Delta V_T(0)$  with edge  $\nabla T$ , both in I-mode and H-mode. Fig. 6 shows the result, with H-mode points as dots and I-mode points as \*. As is evident,  $\Delta V_T(0)$  tracks  $\nabla T$  fairly well, in both H-mode and I-mode. This clearly suggests that the edge or pedestal temperature gradient is the drive of intrinsic rotation. Ongoing work is focused on a study of the relation  $\Delta V_T(0) \sim \nabla T/B_\theta|_{edge}$  as an alternative scaling expressed in terms of local quantities, and on the correlation of edge electric field shear with  $\Delta V_T(0)$ . We note here that the high density regime of C-Mod makes it impossible to separate  $T_e$  from  $T_i$ . Thus, the driving gradient could be either  $\nabla T_e$  or  $\nabla T_i$ , depending of the nature of the turbulence (i.e. CTEM or ITG). To this end, its useful to recall that gyrokinetic particle simulations[6] have shown that intrinsic rotation in ITG turbulence correlates with  $\nabla T_i$  while in CTEM turbulence, it correlates with  $\nabla T_e$ . Either is possible in C-Mod, and the ultimate resolution of the question requires detailed edge fluctuation measurements.

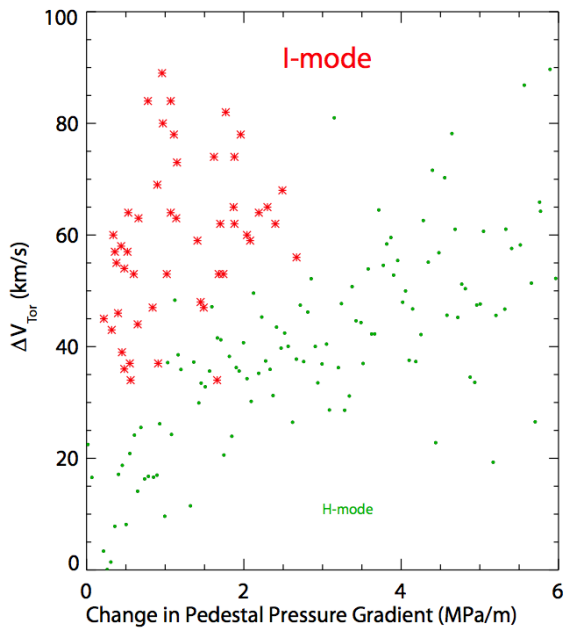


Figure 5: The change in the core rotation velocity as a function of the change in the pedestal electron *pressure* gradient for H-mode (green dots) and I-mode (red asterisks) plasmas.

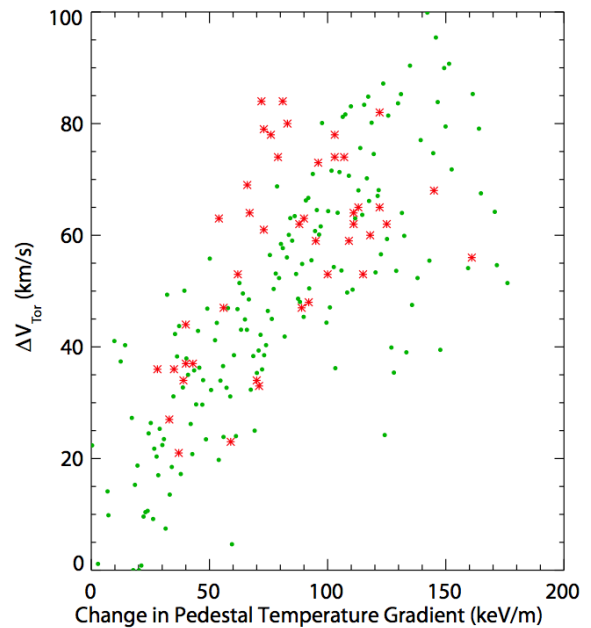


Figure 6: The change in the core rotation velocity as a function of the change in the pedestal electron *temperature* gradient for H-mode (green dots) and I-mode (red asterisks) plasmas.

### 3. Microscopics: CSDX

We now shift attention from macroscopic scaling trends to the detailed dynamics of the residual stress. To do this, we turn to fluctuation studies on a well-diagnosed linear device, the Controlled Shear Decorrelation experiment (CSDX), which uses an RF source to generate highly ionized magnetized plasmas in a uniform magnetic field. Device descriptions and study of the transition to a state of collisional drift turbulence can be found elsewhere[7]. An azimuthal plasma fluid drift is maintained in the absence of external momentum input[8]; this flow has been shown to be self-consistent with the measured turbulent Reynolds stress and estimated flow damping[9] and can be thought of as a zonal flow. However, the plasma column has a net azimuthal rotation in the absence of an external momentum source, and thus must interact with the surrounding environment in order to maintain this state. Note that intrinsic azimuthal rotation exceeds the electron diamagnetic velocity.

Theory suggests[10] that the total turbulent stress  $\Pi_{r\theta}^{tot}$  be decomposed into diffusive, convective and residual (or non-diffusive) components as  $\Pi_{r\theta}^{tot} = -\chi_{\theta}\langle V_{\theta}\rangle' + V_r^{eff}\langle V_{\theta}\rangle + \Pi_{r\theta}^{res}$ . In the cylindrical geometry of this experiment we can take  $V_r^{eff} = 0$ . The residual stress can then be inferred by directly measuring the total azimuthal Reynolds stress profile  $\Pi_{r\theta}^{tot} = \langle \tilde{v}_r \tilde{v}_{\theta} \rangle$  with  $\tilde{\mathbf{v}} = (\hat{\mathbf{b}} \times \nabla \phi_f) / B_0$ , and then synthesizing the diffusive turbulent viscous momentum flux  $\Pi_{r\theta}^{diff} = -\langle \tilde{v}_r^2 \tau_c \rangle \langle V_{\theta} \rangle'$  using direct measurements of radial velocity

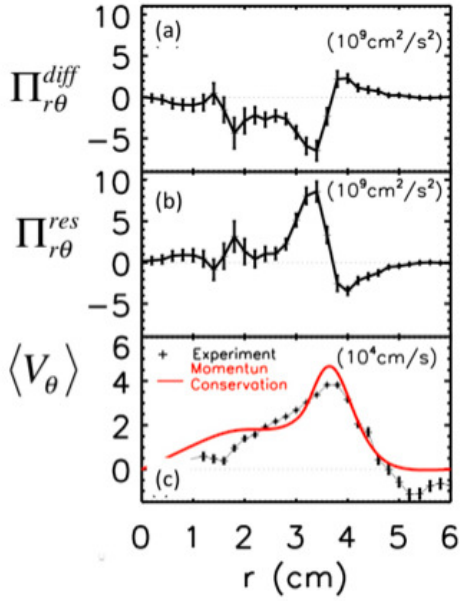


Figure 7: (a) Diffusive stress and (b) residual stress inferred from measured total stress and random walk diffusive momentum transport coefficient. (c) time-averaged plasma flow velocity from measurements (+) and turbulent momentum conservation analysis (solid line).

fluctuations  $\langle \tilde{v}_r^2 \rangle$  and turbulence correlation time  $\tau_c$  and the rotation profile, and then subtracting to isolate the residual stress,  $\Pi_{r\theta}^{res}$  [11]. Results (Figs 7a-b) indicate the presence of a significant residual stress which is most prominent at the plasma edge region located at radius  $r = 3.5 - 4.0 \text{ cm}$ , and which corresponds to an outward flux of positive azimuthal rotation. It is particularly important to note that there is a narrow region of negative divergence for this stress located in the region  $3.5 < r < 4.0 \text{ cm}$ , which will give a Reynolds force  $F_\theta^{Re} = -\nabla_r \Pi_{r\theta}^{res} > 0$  which reinforces the positive azimuthal plasma rotation. The location of this region is coincident with the location of the edge velocity shear layer (Fig. 7c). The diffusive stress (Fig. 7b) is significant in the region  $r < 3 \text{ cm}$ , and corresponds to an inward transport of positive azimuthal rotation. The total stress, combined with flow damping estimates then results in the time-averaged azimuthal flow profile shown as the solid red line in Fig. 7c, which is in reasonable agreement with the measurements, also shown in the figure.

The sheared flow has also been found to slowly (over 1-2msec) increase and then collapse rapidly. Focusing on the growth phase of the flow (Fig. 8), we observe that the flow increase appears to originate in the  $3 < r < 4 \text{ cm}$  region, consistent with the time-averaged results discussed above. The core plasma then spins up in response to the

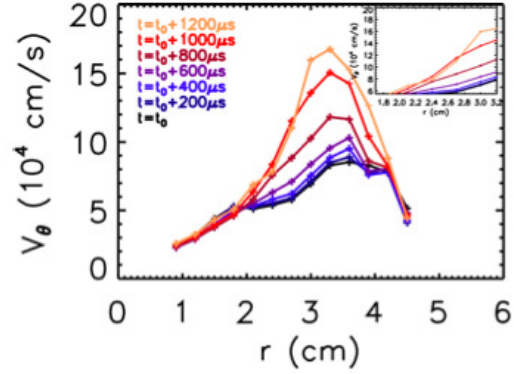


Figure 8: A slow variation (1 – 2msec) in the azimuthal rotation rate and shearing rate occurs. The flow appears to build up in the region between  $r = 3 - 4 \text{ cm}$ , consistent with a mechanism that drives flow in this annular region. The core plasma then nearly maintains solid body rotation in response. Gas pressures are lower in these experiments, resulting in higher values for azimuthal rotation than for conditions of Fig. 7.

increased rotation in this outer annular region. We estimate that the turbulent and collisional momentum diffusion result in a radial turbulent momentum diffusion timescale  $\tau_{\theta}^{diff} = a^2/(\mu_{ii} + \chi_{\theta}) = 50 - 100\mu sec$ , which is not inconsistent with the flow profile evolution shown in Fig. 8. Strong on-axis neutral density depletion (by a factor  $\sim T_{gas}(r=0)/T_{gas}(r=r_{wall}) \sim 35$ ) occurs in these discharge conditions yielding a central plasma ion-neutral damping timescale  $\tau_{io} = 1/(n_{gas}\sigma_{io}^{tot}V_{\theta}) \cong 200\mu sec$ . The combined effects of turbulent and collisional momentum diffusion and weaker ion-neutral damping, then dominate the residual stress for  $r < 3cm$ , and act to couple the residual stress-driven sheared edge flow in the  $3 < r < 4cm$  region with the central plasma on the  $\tau_{\theta}^{diff}$  timescale. Outside the plasma boundary the neutrals are nearly in thermal equilibrium with the wall located at  $r = 10cm$  and must therefore have a density of  $1014cm^{-3}$  from the measured gas pressure. Ion-neutral momentum exchange then gives a mean free path  $\lambda_{io}^{mfp}|_{r>a} = 1/(n_{gas}\sigma_{io}^{tot})|_{r>a} \cong 0.1cm$  in this region. Thus in the outer regions the ion-neutral flow damping imposes an effective a no-slip boundary condition  $\tilde{V}_{\theta}|_{r>r'}$  at a radius  $r' > a$  lying in the outer plasma region where the ion density is small.

These results indicate that a residual turbulent stress can act on the plasma boundary to sustain and amplify the plasma flow in this region. Inward diffusion of this momentum then couples this annular flow to the central plasma region; the plasma column can then acquire a net rotation through the imposition of a no-slip boundary condition in the outer regions due to strong ion-neutral flow coupling in this region. These observations are qualitatively similar to observations of intrinsic rotation in toroidal devices, and provide an opportunity to make detailed tests of theoretical models of this phenomena. In particular, here we have established the viability of the concept of fluctuation induced residual stress.

#### 4. Theory: Intrinsic Rotation as Engine

We now turn from macro and micro experiments to theory, and propose a theoretical framework for the intrinsic rotation phenomena. This framework is cast in terms of fluctuation entropy and describes intrinsic rotation as a thermodynamic engine. In the framework of residual stress, the generation process of flows can be understood as a conversion of thermal energy, which is injected into a system by heating, into kinetic energy of macroscopic flow by drift wave turbulence excited by  $\nabla T$ ,  $\nabla n$ , etc. In this section, using the physical picture of flow generation as a energy conversion, we formulate an explicit expression for the criterion for *efficiency* of the conversion process by comparing *rates of entropy production/destruction* due to thermal relaxation/flow generation.[12]

For a simple model with drift kinetic ions and adiabatic electrons, the time evolution of entropy or  $\delta f^2$  is given by

$$\begin{aligned} & \partial_t \int d\Gamma \frac{\langle \delta f^2 \rangle}{\langle f \rangle} \\ &= \int d^3x \left\{ -\frac{n}{T_i L_T} Q_{turb}^i - \frac{n}{v_{thi}^2} \langle V_{\perp} \rangle' \langle \tilde{V}_r \tilde{V}_{\perp} \rangle - \frac{n}{v_{thi}^2} \langle V_{\parallel} \rangle' \langle \tilde{V}_r \tilde{V}_{\parallel} \rangle + \frac{1}{T_i} \langle \tilde{J}_{\parallel}^i \tilde{E}_{\parallel} \rangle \right\} \quad (1) \end{aligned}$$

apart from collisional dissipation and boundary terms. The right hand side can be further simplified for a stationary state. Using a simple model for turbulent flux and neglecting

pinch, we have

$$P \equiv \int d^3x \left\{ n\chi_i \left( \frac{\nabla T}{T} \right)^2 - nK \left( \frac{\langle V_E \rangle'}{v_{thi}} \right)^2 + n\chi_\phi \left( \frac{\langle V_{\parallel} \rangle'}{v_{thi}} \right)^2 - n \frac{\Pi_{r\parallel}^{res2}}{v_{thi}^2 \chi_\phi} \right\} \quad (2)$$

where  $K \equiv \sum_k c_s^2 \tau_{ZF} (\rho_s^2 k_\theta^2) / (1 + k_\perp^2 \rho_s^2) \{-k_r \partial \eta_k / \partial k_r\}$ ,  $\eta_k \equiv (1 + k_\perp^2 \rho_s^2)^2 |\hat{\phi}_k|^2$ . The first term in the right hand side is the entropy production rate due to thermal relaxation. The second term is the entropy destruction rate due to zonal flow generation. Note that this term destructs entropy only when zonal flow grows, i.e.  $\gamma_{ZF} \propto K > 0$ . The third term is the entropy production rate due to the relaxation of velocity gradient. The last term is the entropy destruction rate due to the generation of intrinsic toroidal rotation.

The production rate  $P$  contains terms with a definite order. The last two terms are smaller than the first two terms by the order of  $O(k_{\parallel}/k_{\perp})$  where  $k$  is a representative of the mode number of drift waves. Hence a stationary state is achieved by balancing the production and destruction rates order by order. To the lowest order, we have the balance between the production rate from thermal relaxation and the destruction rate from zonal flow growth. The balance yields  $\langle V_E \rangle'^2 = (\chi_i/K)(v_{thi}^2/L_T^2)$  which relates zonal flow strength to the temperature gradient directly. To the next order, the third and the fourth term in Eq. 2 cancels since the total parallel momentum vanishes for a stationary state as  $\langle \tilde{V}_r \tilde{V}_{\parallel} \rangle = -\chi_\phi \langle V_{\parallel} \rangle' + \Pi_{r\parallel}^{res} = 0$ .

We can define a figure of merit or an efficiency of intrinsic rotation generation process, by comparing the entropy production rate and destruction rate discussed above. Only keeping the dominant production rate in the denominator, we have

$$e_{IR} \cong \frac{\int d^3x n (\Pi_{r\parallel}^{res})^2 / (v_{thi}^2 \chi_\phi)}{\int d^3x n \chi_i (\nabla T/T)^2} \quad (3)$$

Note that this relation gives an upper bound for the efficiency, since we dropped entropy production rates from other relaxation processes such as collisions, which are small compared to production rates due to turbulent thermal relaxation.

To calculate an actual scaling, we need modeling of the residual stress. Here, we consider a case where toroidal rotation is driven by a two step process: first, a stationary state is achieved by balancing the entropy production rate due to thermal relaxation by the entropy destruction due to zonal flow growth. Secondary, the zonal flow  $E \times B$  shear set by the dominant balance gives rise to symmetry breaking and momentum flux via  $k$  space scattering. In such a process, the residual stress is calculated as

$$\Pi_{r\parallel}^{res} = -\rho_* \frac{L_s}{2c_s} K \langle V_E \rangle'^2 = -\rho_* \frac{L_s}{2c_s} \chi_i \left( \frac{\nabla T}{T} \right)^2 v_{thi}^2 \quad (4)$$

and the efficiency can be calculated further and shown to be

$$e_{IR} = \frac{\int d^3x n \frac{\chi_i}{\chi_\phi} \chi_i (\nabla T/T)^2 \frac{L_s^2 \rho_*^2 v_{thi}^2}{L_T^2 4 c_s^2}}{\int d^3x n \chi_i (\nabla T/T)^2} \sim \rho_*^2 \frac{q^2}{\hat{s}^2} \frac{R^2}{L_T^2} \quad (5)$$

where we assumed that  $\chi_i \sim \chi_\phi$ ,  $T_e \sim T_i$ ,  $\hat{s} \neq 0$ . The efficiency of intrinsic toroidal flow generation scale as machine size  $\rho_*$ , geometry of the B field  $q/\hat{s}$  and temperature profile  $R/L_T$ . The efficiency exhibits a similar scaling behavior to the Rice scaling, except for the appearance of explicit  $\rho_*$  scaling. Note that the efficiency scaling suggests a possible origin of the unfavorable current scaling through the safety factor  $q$ , or perhaps, the magnetic shear  $\hat{s}$ [13]. Here, it is worthwhile to comment that the strong scaling of the residual stress with  $\nabla T/T$  (see Eq. 4) is entirely consistent with the observed  $\Delta V_T(0)$  vs  $\nabla T|_{ped}$  correlation discussed earlier. Also, the condition  $\Pi_{r\parallel} = 0$  implies a strongly nonlinear relation between  $\nabla V_\phi$  and  $\nabla T/T$ , i.e.  $\partial\langle V_\phi \rangle/\partial r \cong -\rho_*(L_s/2c_2)(\chi_i/\chi_\phi)(\nabla T/T)^2 v_{thi}^2$ . Simple integration then establishes a nonlinear relation between edge  $\nabla T$  and  $V_T(0)$ , also observed in experiments. Finally, we remind the reader that all the calculations here assume  $\hat{s} > 0$ .

## 5. Conclusion

In this paper, we have described progress toward a physics based phenomenology of intrinsic rotation in H-mode and I-mode. The principal results of this paper are as follows.

1. studies in Alcator C-Mod indicate a close correlation between change in central velocity  $\Delta V_T(0)$  and  $\nabla T|_{edge}$ , both in H-mode and I-mode. This, in turn, suggests that the macroscopic scaling  $\Delta V_T(0) \sim \Delta W_p/I_p$  may be replaced by a relation expressed in terms of *local* parameters i.e.  $\Delta V_T(0) \sim \nabla T/B_\theta$ . Central velocity does not correlate with edge  $\nabla p$  in the I-mode.
2. studies in the CSDX linear device demonstrate the existence and role of a non-diffusive stress which is sufficient to drive intrinsic rotation, acting through a no-slip boundary condition, enforced by high neutral density.
3. a theory of the entropy balance for a turbulent plasma is presented, which yields a figure of merit for the efficiency of the intrinsic rotation engine. The theory predicts that the both the efficiency and  $V_T(0)$  scale strongly with  $\nabla T/T$ .

## References

- [1] Gürçan, Ö.D., *et al.*, Phys. Plasmas, **14**, 042306 (2007)
- [2] Biglari, H., *et al.*, Phys. Fluids B, **2**, 1 (1990)
- [3] Whyte, D.G., *et al.*, Nucl. Fusion, **50**, 105005, (2010)
- [4] Rice, J.E., *et al.*, Nucl. Fusion, **47**, 1618 (2007)
- [5] Rice, J.E., *et al.*, Nucl. Fusion, **44**, 379 (2004)
- [6] Wang, W.X., *et al.*, accepted to Phys. Plasmas (2010)
- [7] Burin, M.J., *et al.*, Phys. Plasmas **12**, 14 (2005)
- [8] Yu, J.H., *et al.*, J. Nucl. Mater. **363**, 728 (2007)
- [9] C. Holland *et al.*, Phys. Rev. Lett. **96**, 195002 (2006)
- [10] Diamond, P.H., *et al.*, Nucl. Fusion **49**, 045002 (2009)
- [11] Yan, Z., *et al.*, Phys. Rev. Lett. **104**, 065002 (2010)
- [12] Kosuga, Y., *et al.*, Phys. Plasmas, in press (2010)
- [13] Kwon, J.-M., this conference (2010)